Figure 1

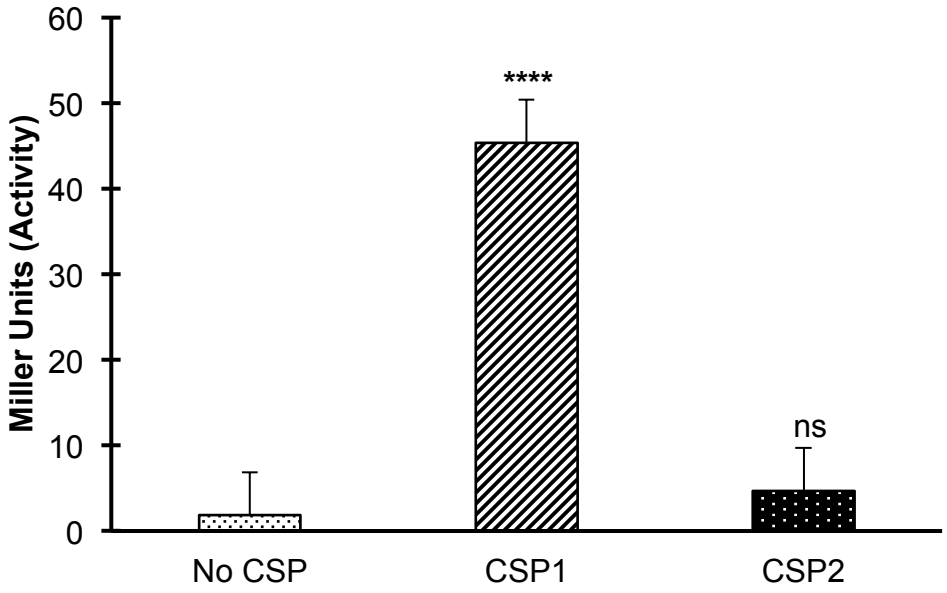

Fig. 1. Expression of *briC* is induced by cognate CSP. β-galactosidase assay measuring P*briC*-lacZ activity in pneumococcal R6 cells grown to exponential phase in Columbia Broth at pH 6.6 followed by no treatment or treatment with CSP1 or CSP2 for 30 minutes. Y-axis denotes P*briC-lacZ* expression levels in Miller Units. Activity is expressed in nmol p-nitrophenol/min/ml. Error bars represent standard error of the mean for biological replicates *(at least n=3)*; **** $p<0.0001$ using ANOVA followed by Tukey's post-test.

Figure 2

(A)

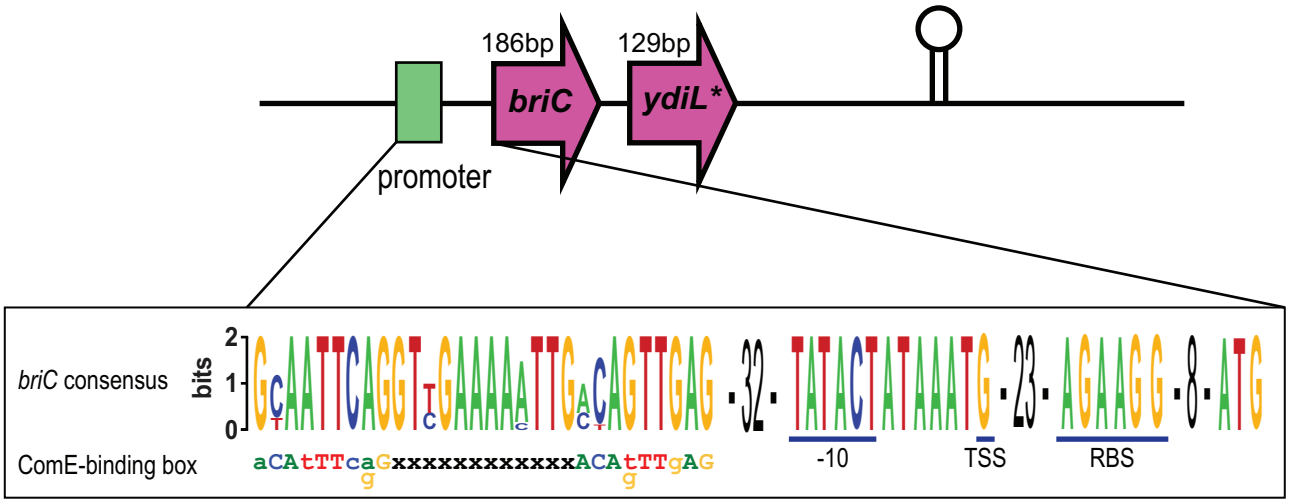
186bp
129bp
briC
ydiL*
promoter
briC consensus
bits
2
1
0
-32-
-23-
-8-
ATG
ComE-binding box
aCAtTTcaGxxxxxxxxxxxxxACAtTTgAG
-10
TSS
RBS

Figure 2

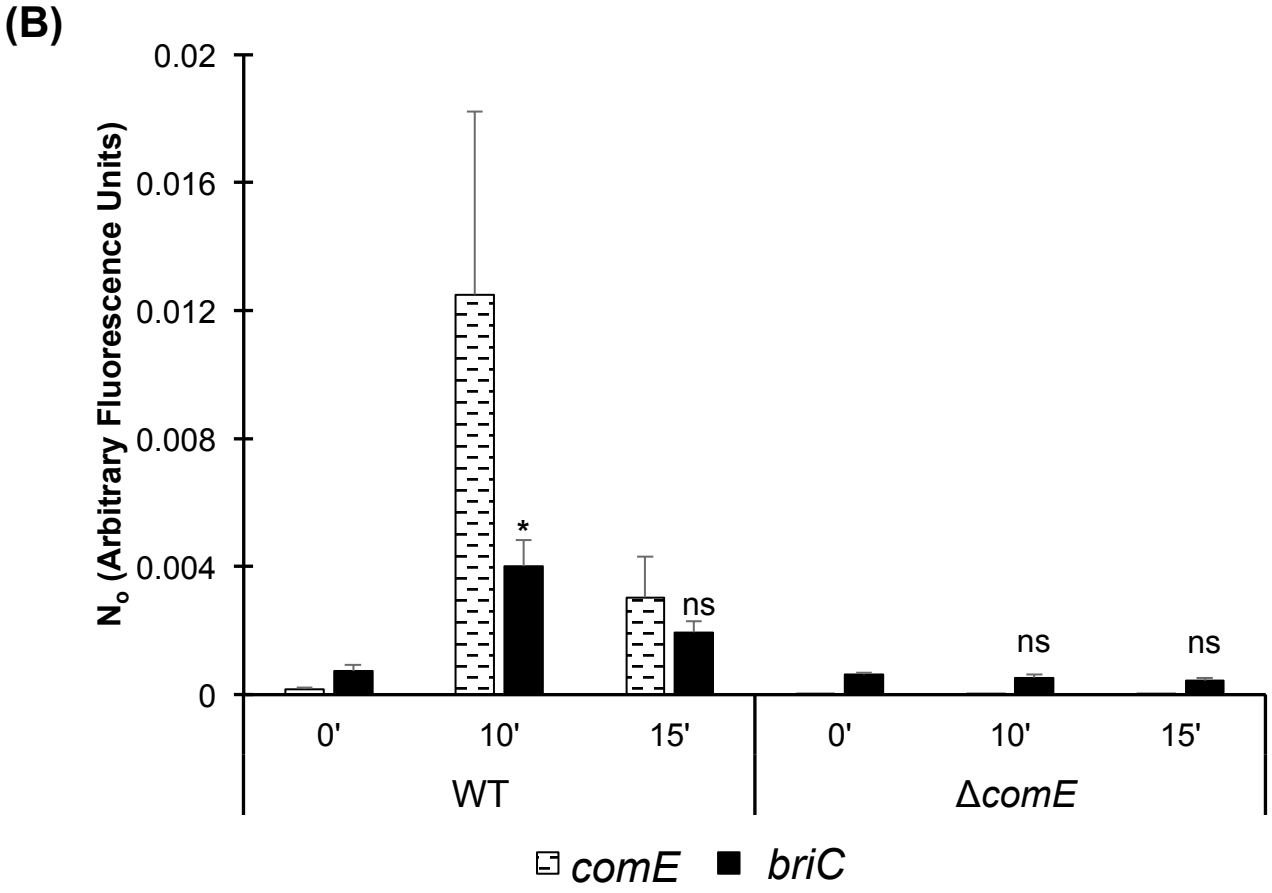

Fig. 2. **CSP-induction of *briC* is ComE-dependent**. (A) Genomic organization of the *briC* locus, displaying a ComE-binding box. Green: ComE-binding box within the *briC* promoter region. The expanded region denotes a logo of ComE-binding box generated from thirty-four pneumococcal genomes represented in Figure 4A. This consensus is aligned with the published ComE-binding box consensus sequence (Ween et al., 1999). The putative -10 region, the **t**ranscription **s**tart **s**ite (TSS), the **r**ibosome **b**inding **s**ite (RBS) and the transcriptional terminator are labeled. The downstream gene is predicted to be a pseudogene in R6D, R6 and D39. In TIGR4, this region encodes two coding sequences (SP_0430 and SP_0431). The R6D sequence corresponds to the C-terminal of SP_0430. (B) mRNA transcript levels of *briC* (solid black) and *comE* (dashed black lines) as measured by qRT-PCR in R6D WT & R6DΔ*comE* cells. Cells were grown in Columbia broth at pH 6.6 to an OD_{600} of 0.3, and then treated with CSP1 for either 0', 10' or 15'. Data was normalized to 16S rRNA levels. Y-axis denotes normalized concentrations of mRNA levels in arbitrary fluorescence units as calculated from LinRegPCR. Error bars represent standard error of the mean calculated for biological replicates *(n=3)*; 'ns' denotes non-significant, * $p<0.05$ using ANOVA followed by Tukey's post-test relative to the respective 0' CSP treatment. Further, *briC* levels are also significantly higher in WT relative to Δ*comE* cells for the same time points post-CSP treatment ($p<0.05$).

Figure 3

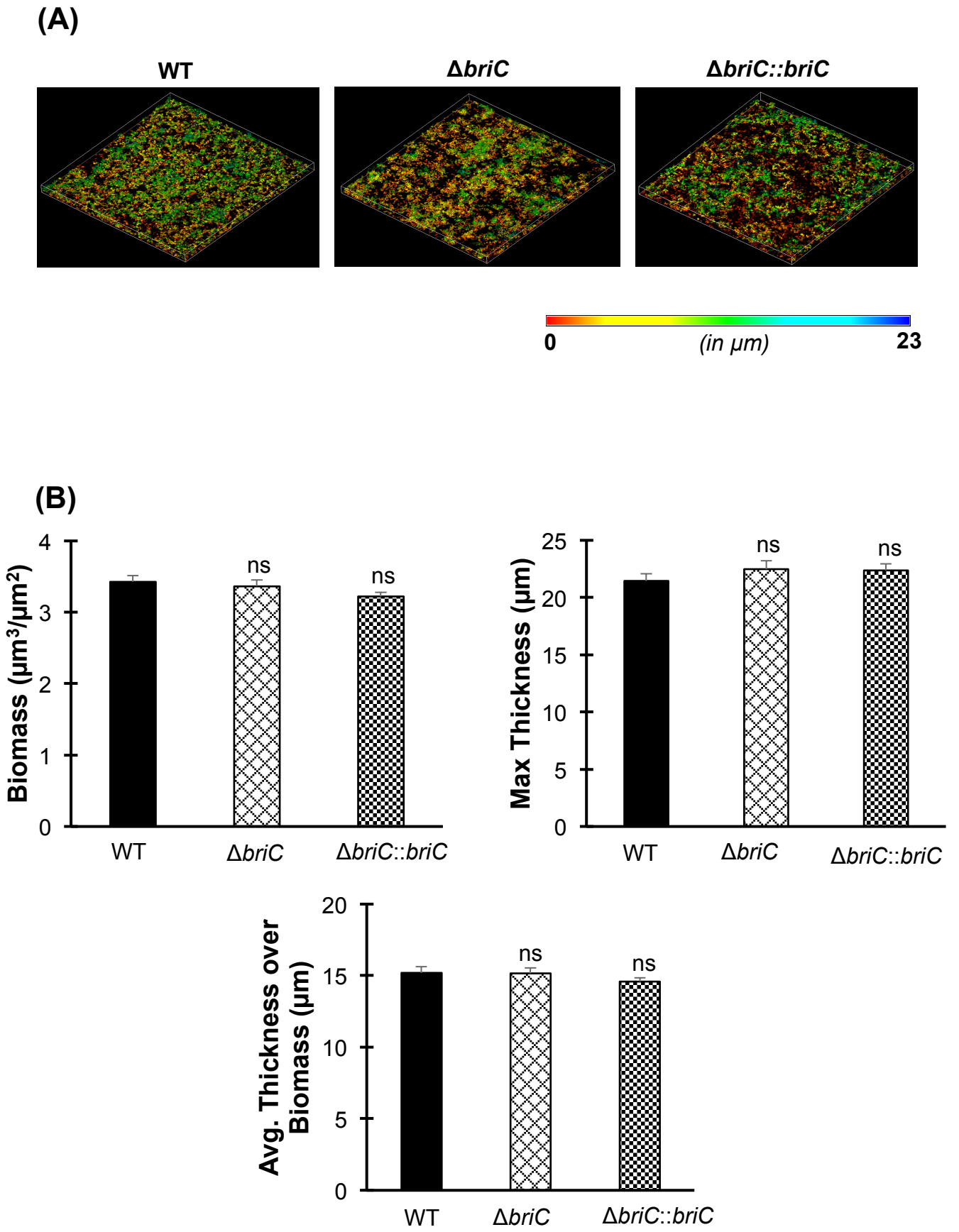
(A)
WT
ΔbriC
ΔbriC::briC
0
(in µm)
23
(B)
Biomass (µm³/µm²)
4
3
2
1
0
ns
ns
WT
ΔbriC
ΔbriC::briC
Max Thickness (µm)
25
20
15
10
5
0
ns
ns
WT
ΔbriC
ΔbriC::briC
Avg. Thickness over Biomass (µm)
20
15
10
5
0
ns
ns
WT
ΔbriC
ΔbriC::briC

Figure 3

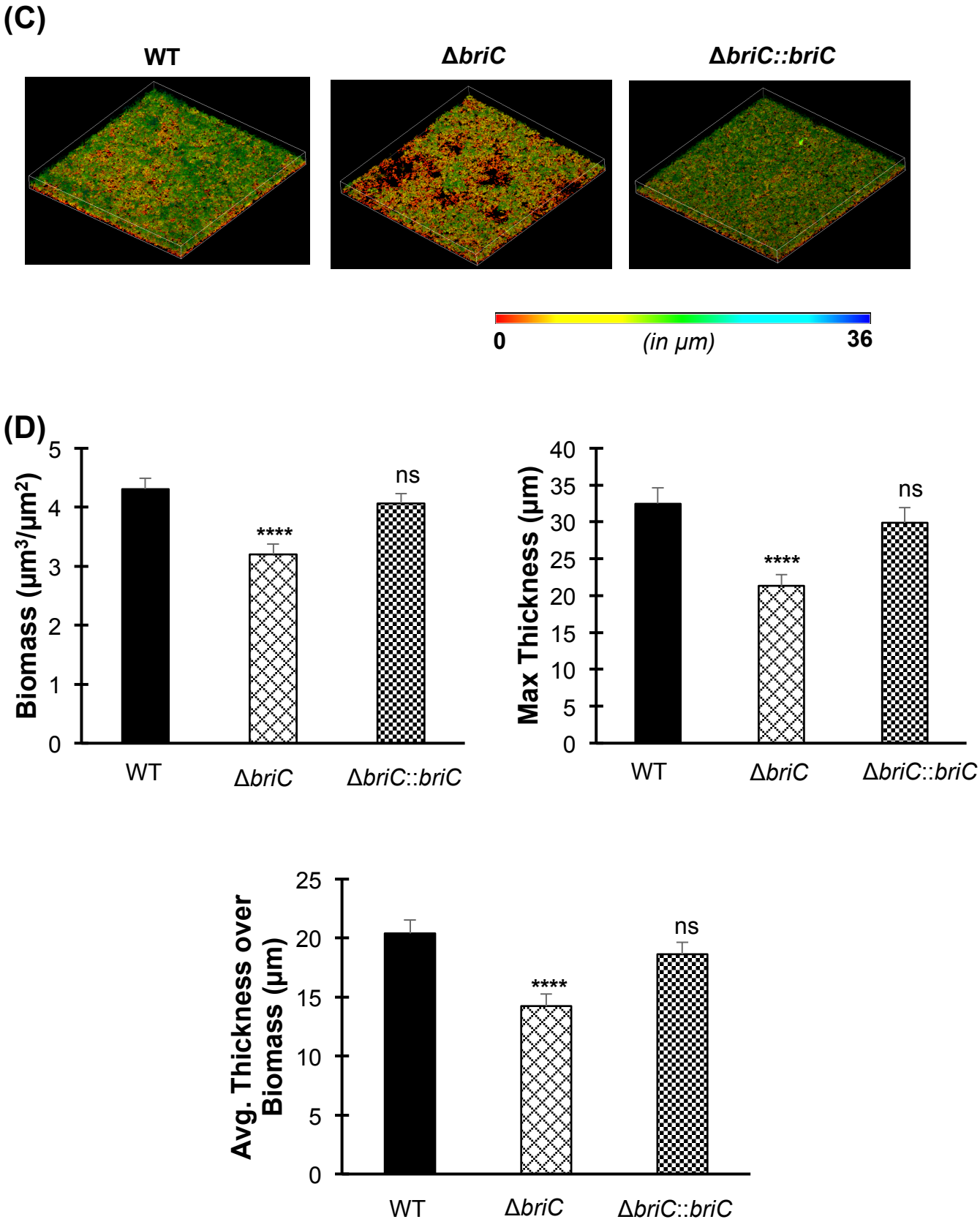
(C)
WT
ΔbriC
ΔbriC::briC
0
(in μm)
36
(D)
Biomass (μm³/μm²)
5
4
3
2
1
0
****
ns
WT
ΔbriC
ΔbriC::briC
Max Thickness (μm)
40
35
30
25
20
15
10
5
0
****
ns
WT
ΔbriC
ΔbriC::briC
Avg. Thickness over Biomass (μm)
25
20
15
10
5
0
****
ns
WT
ΔbriC
ΔbriC::briC

Fig. 3. BriC stimulates late biofilm development. Representative confocal microscopy images showing top view of the reconstructed biofilm stacks of WT, Δ*briC* and Δ*briC::briC* cells of strain R6D stained with SYTO59 dye at **(A)** 24-hr, and **(C)** 72-hr. Images are pseudo-colored according to depth (scales shown). COMSTAT2 quantification of **(B)** 24-hr, and **(D)** 72-hr biofilm images. Y-axis denotes units of measurement: $\mu m^3/\mu m^2$ for biomass, and μm for maximum thickness and average thickness over biomass. Error bars represent standard error of the mean calculated for biological replicates *(n=3)*; "ns" denotes non-significant comparisons, **** $p<0.0001$ using ANOVA followed by Tukey's post-test.

Figure 4

(A)

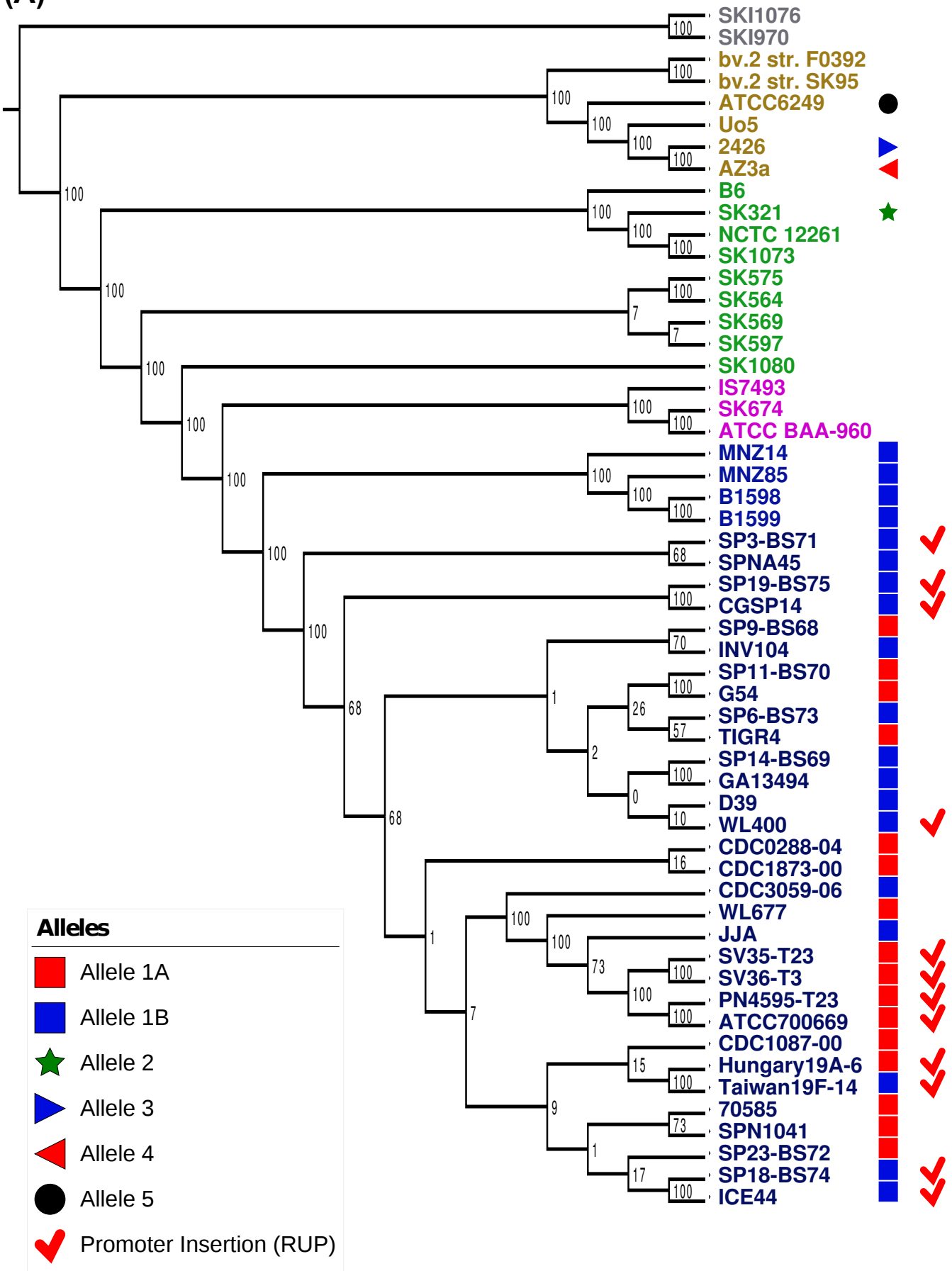
SKI1076
SKI970
bv.2 str. F0392
bv.2 str. SK95
ATCC6249
Uo5
2426
AZ3a
B6
SK321
NCTC 12261
SK1073
SK575
SK564
SK569
SK597
SK1080
IS7493
SK674
ATCC BAA-960
MNZ14
MNZ85
B1598
B1599
SP3-BS71
SPNA45
SP19-BS75
CGSP14
SP9-BS68
INV104
SP11-BS70
G54
SP6-BS73
TIGR4
SP14-BS69
GA13494
D39
WL400
CDC0288-04
CDC1873-00
CDC3059-06
WL677
JJA
SV35-T23
SV36-T3
PN4595-T23
ATCC700669
CDC1087-00
Hungary19A-6
Taiwan19F-14
70585
SPN1041
SP23-BS72
SP18-BS74
ICE44
Alleles
Allele 1A
Allele 1B
Allele 2
Allele 3
Allele 4
Allele 5
Promoter Insertion (RUP)

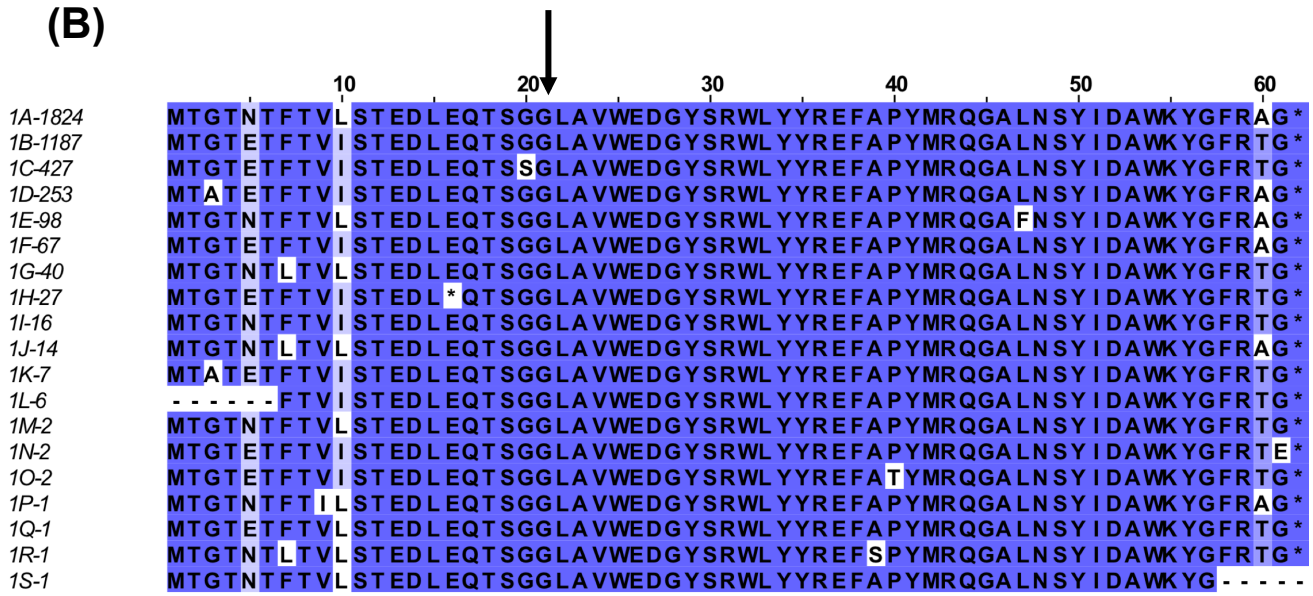

Fig. 4. Distribution of the genomic region encoding BriC across streptococcal strains. (A) Distribution of *briC* alleles in fifty-five streptococcal genomes. The *briC* alleles are visualized against a maximum likelihood tree of streptococcal genomes generated from the core genome, where the numbers on the branches represent bootstrap values. Different species in the tree are color-coded as follows: *S. pneumoniae* (blue), *S. pseudopneumoniae* (pink), *S. mitis* (green), *S. oralis* (beige), and *S. infantis* (grey). The shapes at the tip of the branches illustrate *briC* alleles. Types 1A and 1B represent variants of the alleles widespread across pneumococcal strains; types 3-5 denotes alleles outside the species. The red tick denotes strains that have a longer *briC* promoter due to a RUP insertion. In PMEN1 strains, this variant leads to increase in basal levels of *briC* in a CSP-independent manner. **(B)** Alignment of 19 BriC alleles identified in the database of 4,034 pneumococcal genomes. Alleles are labeled 1A-1S followed by the number of representatives in the database (total 3,976). Sequences are colored based on percent identity to highlight the variability between alleles. Black arrow denotes the predicted cleavage site.

Figure 5

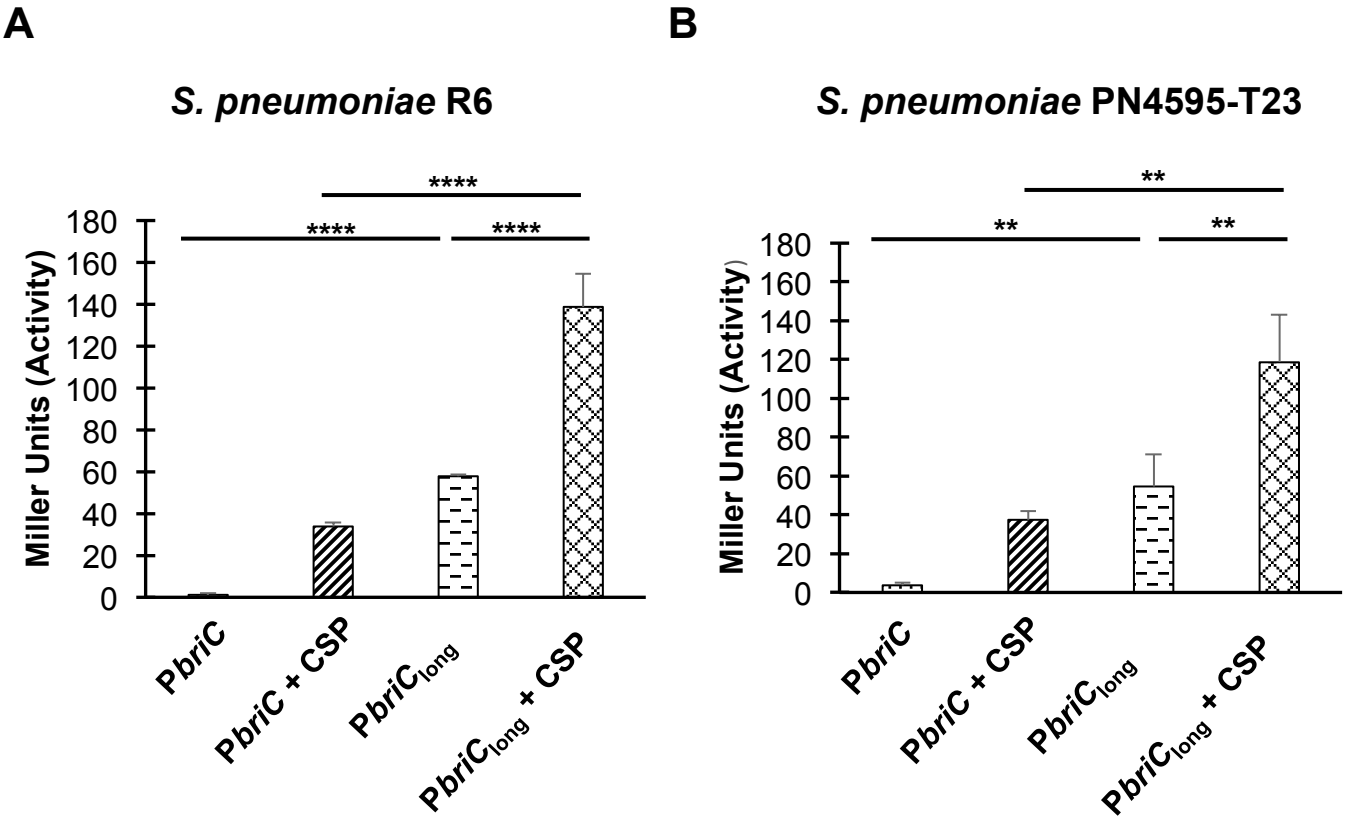

Fig. 5. Longer *briC* promoter is associated with an increase in the basal levels of *briC*. β-galactosidase assay comparing the LacZ activity of the R6 (short promoter, P*briC-lacZ)* and PN4595-T23 (longer promoter with RUP, P$briC_{long}$-*lacZ)* promoters. Both promoter activities were tested in **(A)** strain R6 and **(B)** strain PN4595-T23. Cells were grown in Columbia broth at pH 6.6 until mid-log phase, followed by either no treatment or treatment with CSP for 30 minutes. Y-axis denotes promoter activity in Miller Units expressed in nmol p-nitrophenol/min/ml. Error bars represent standard error of the mean for biological replicates *(n=3)*; ** $p<0.01$, & **** $p<0.0001$ using ANOVA followed by Tukey's post-test.

Figure 6

(A)

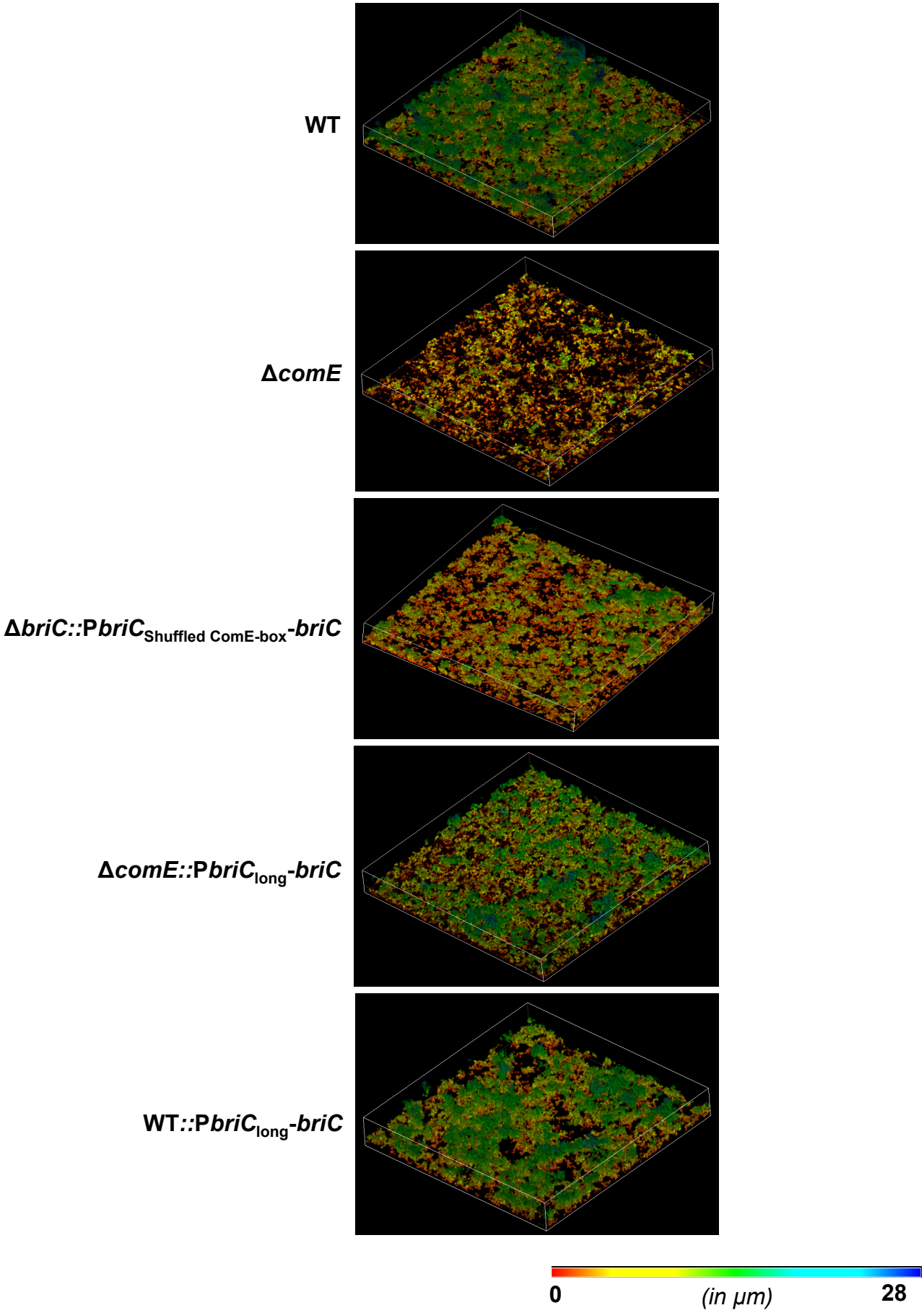
WT
ΔcomE
ΔbriC::PbriCShuffled ComE-box-briC
ΔcomE::PbriClong-briC
WT::PbriClong-briC
0
(in µm)
28

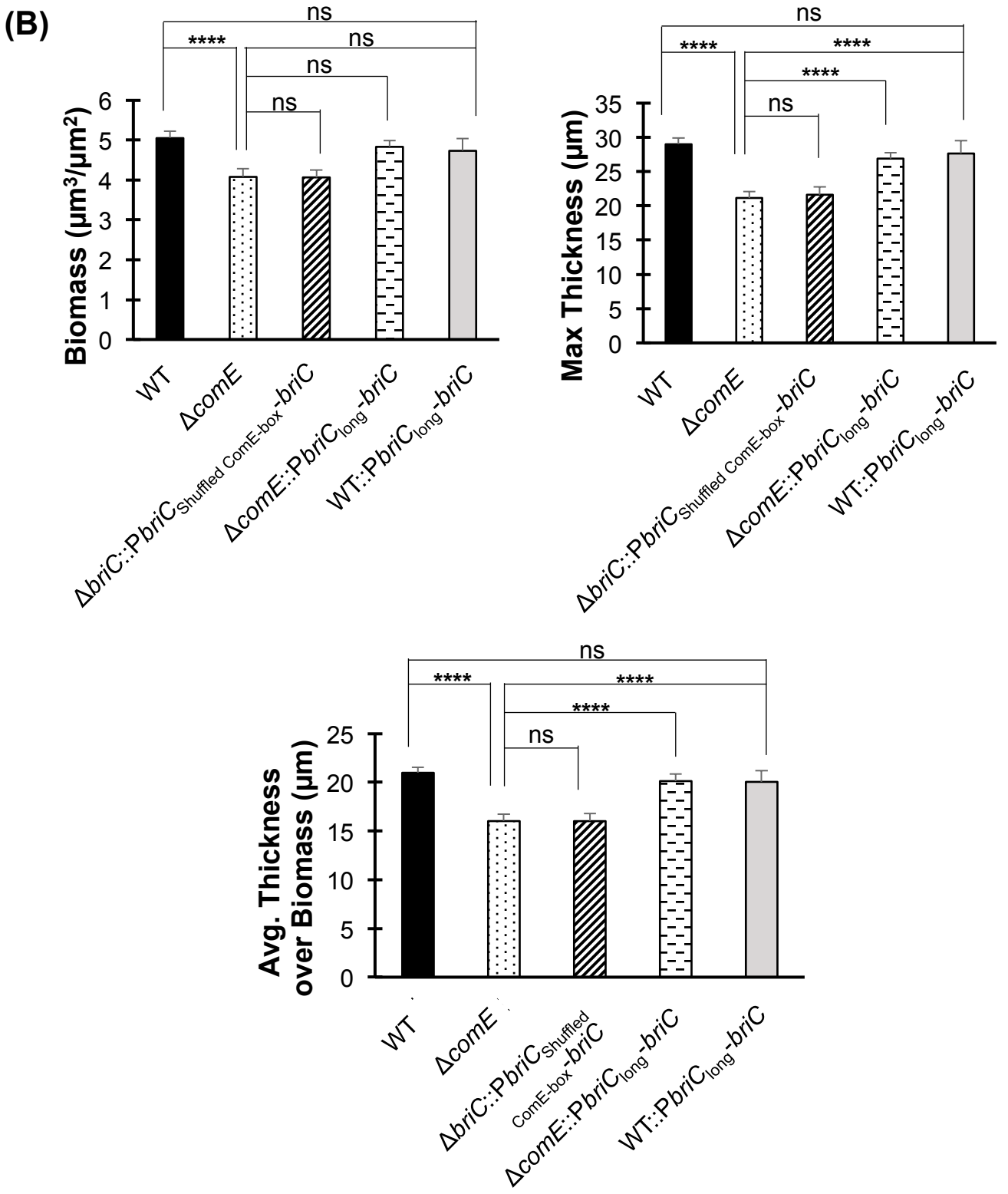

Fig. 6. BriC plays a pivotal role in regulating biofilm development. (A) Representative confocal microscopy images showing top view of the reconstructed biofilm stacks of WT, Δ*comE,* Δ*briC::*P*briC*$_{\text{Shuffled ComE-box}}$-*briC*, Δ*comE::*P*briC*$_{\text{long}}$-*briC* and WT*::*P*briC*$_{\text{long}}$-*briC* cells of strain R6D stained with SYTO59 dye at 72-hr. Images are pseudo-colored according to depth (scale shown). **(B)** COMSTAT2 quantification of 72-hr biofilm images. Y-axis denotes units of measurement: μm^3/μm^2 for biomass, and μm for maximum thickness and average thickness over biomass. Error bars represent standard error of the mean calculated for biological replicates *(at least n=3)*; "ns" denotes non-significant comparisons, and **** $p<0.0001$ using ANOVA followed by Tukey's post-test.

Figure 7

(A)

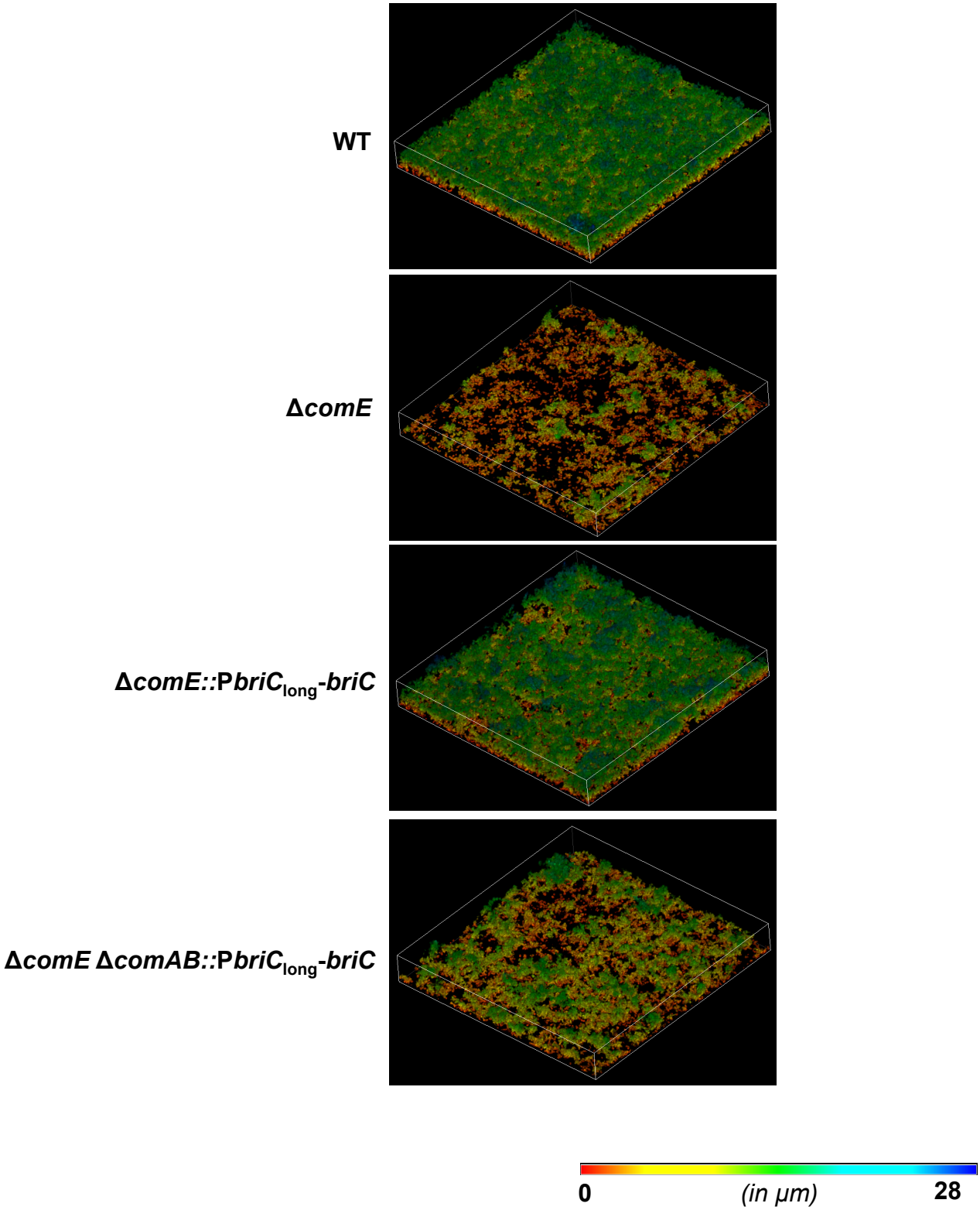
WT
ΔcomE
ΔcomE::PbriC$_{long}$-briC
ΔcomE ΔcomAB::PbriC$_{long}$-briC
0
(in μm)
28

(B)

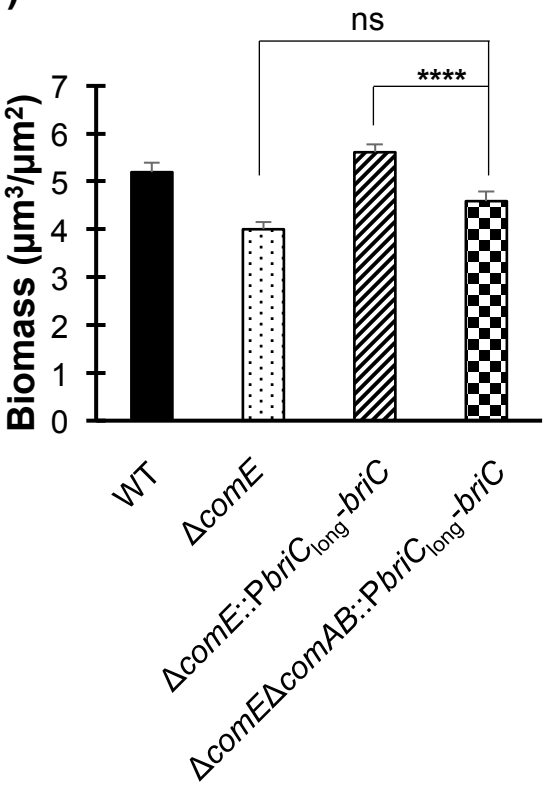
ns
****
Biomass (µm³/µm²)
0
1
2
3
4
5
6
7
WT
ΔcomE
ΔcomE::PbriClong-briC
ΔcomEΔcomAB::PbriClong-briC

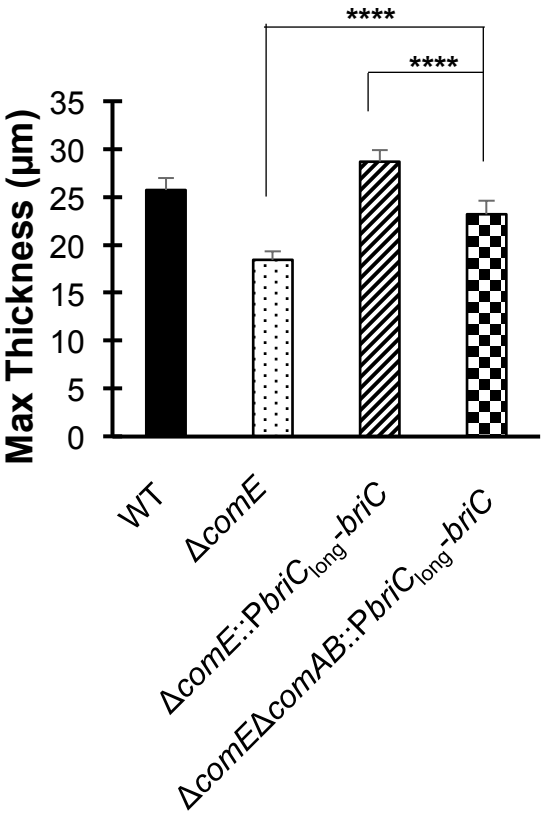
****
****
Max Thickness (µm)
0
5
10
15
20
25
30
35
WT
ΔcomE
ΔcomE::PbriClong-briC
ΔcomEΔcomAB::PbriClong-briC

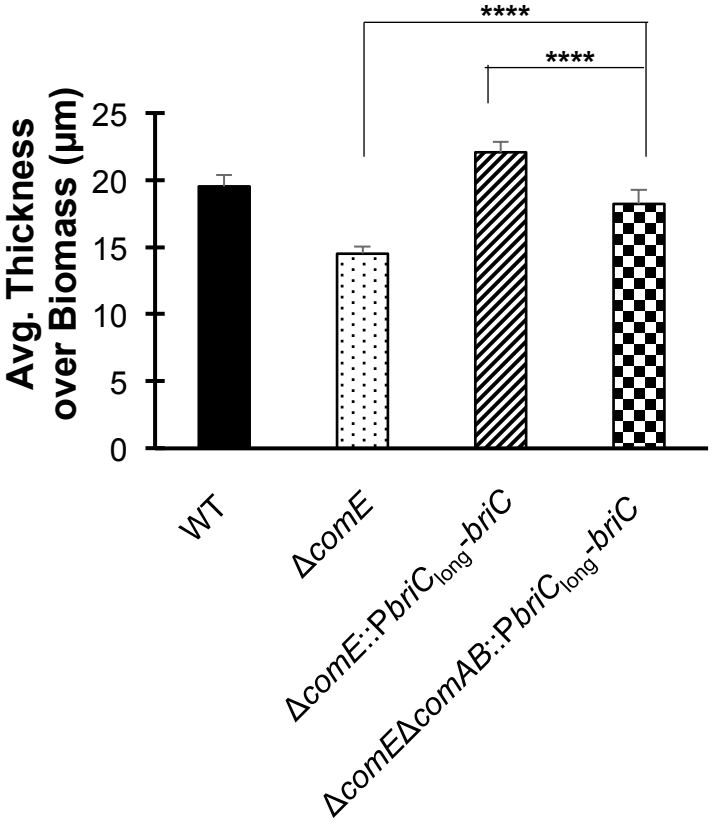
****
****
Avg. Thickness over Biomass (µm)
0
5
10
15
20
25
WT
ΔcomE
ΔcomE::PbriClong-briC
ΔcomEΔcomAB::PbriClong-briC

(C)

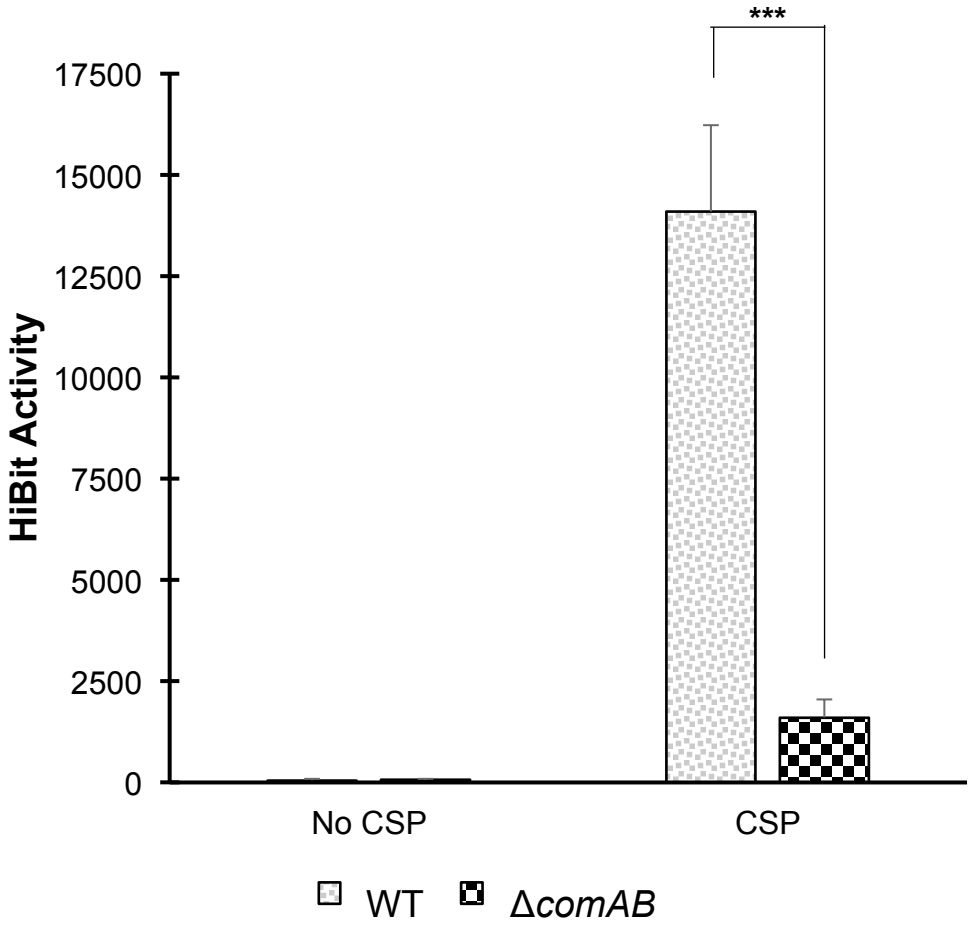

Fig. 7. ComAB plays a role in the export of BriC. (A) Representative confocal microscopy images showing top view of the reconstructed biofilm stacks of WT, Δ*comE,* Δ*comE::*P*briC*$_{long}$-*briC* and Δ*comE*Δ*comAB::*P*briC*$_{long}$-*briC* cells of strain R6D stained with SYTO59 dye at 72-hr. Images are pseudo-colored according to depth (scale shown). **(B)** COMSTAT2 quantification of 72-hr biofilm images. Y-axis denotes units of measurement: $\mu m^3/\mu m^2$ for biomass, and μm for maximum thickness and average thickness over biomass. Error bars represent standard error of the mean calculated for biological replicates *(atleast n=3).* **(C)** Extracellular Nano-Glo HiBit activity of the BriC reporter produced by WT and Δ*comAB* cells (whole cells). The HiBit activity was measured by recording luminescence with an integration time of 2000 milliseconds. Error bars represent standard deviation calculated for biological replicates *(n=3)*; "ns" denotes non-significant comparisons, *** $p<0.001$, and **** $p<0.0001$ using ANOVA followed by Tukey's post-test.

Figure 8

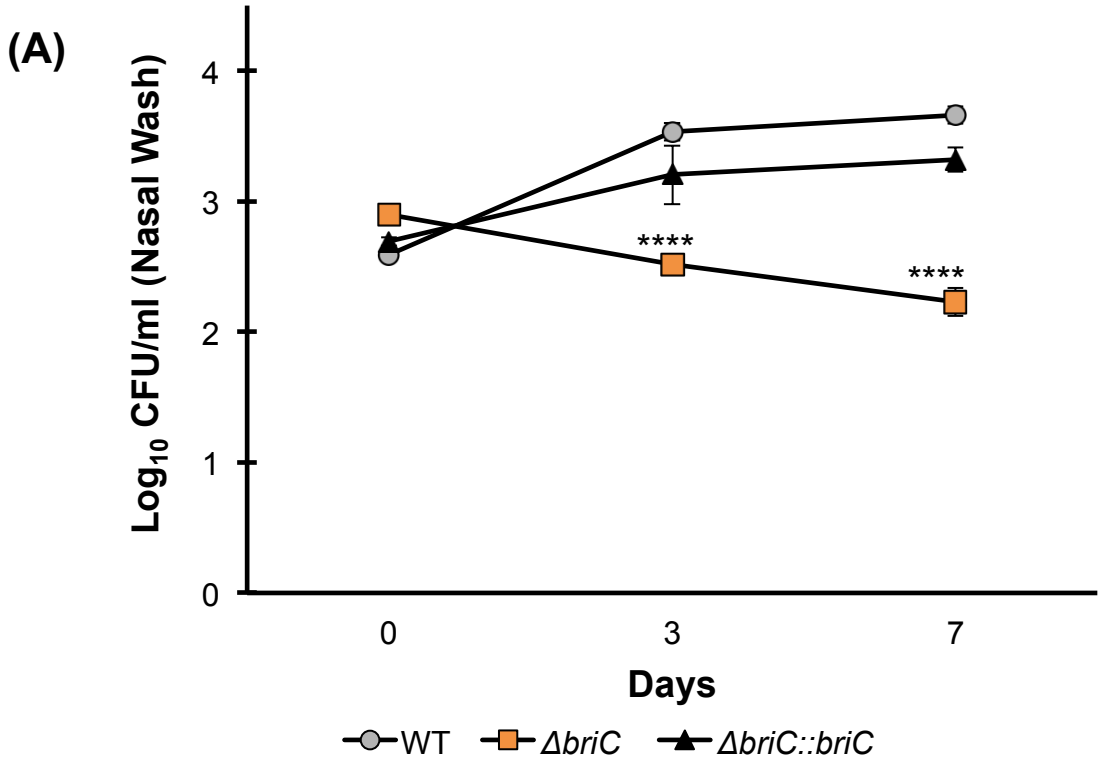
(A)
Log10 CFU/ml (Nasal Wash)
4
3
2
1
0
****
****
0
3
7
Days
WT
ΔbriC
ΔbriC::briC

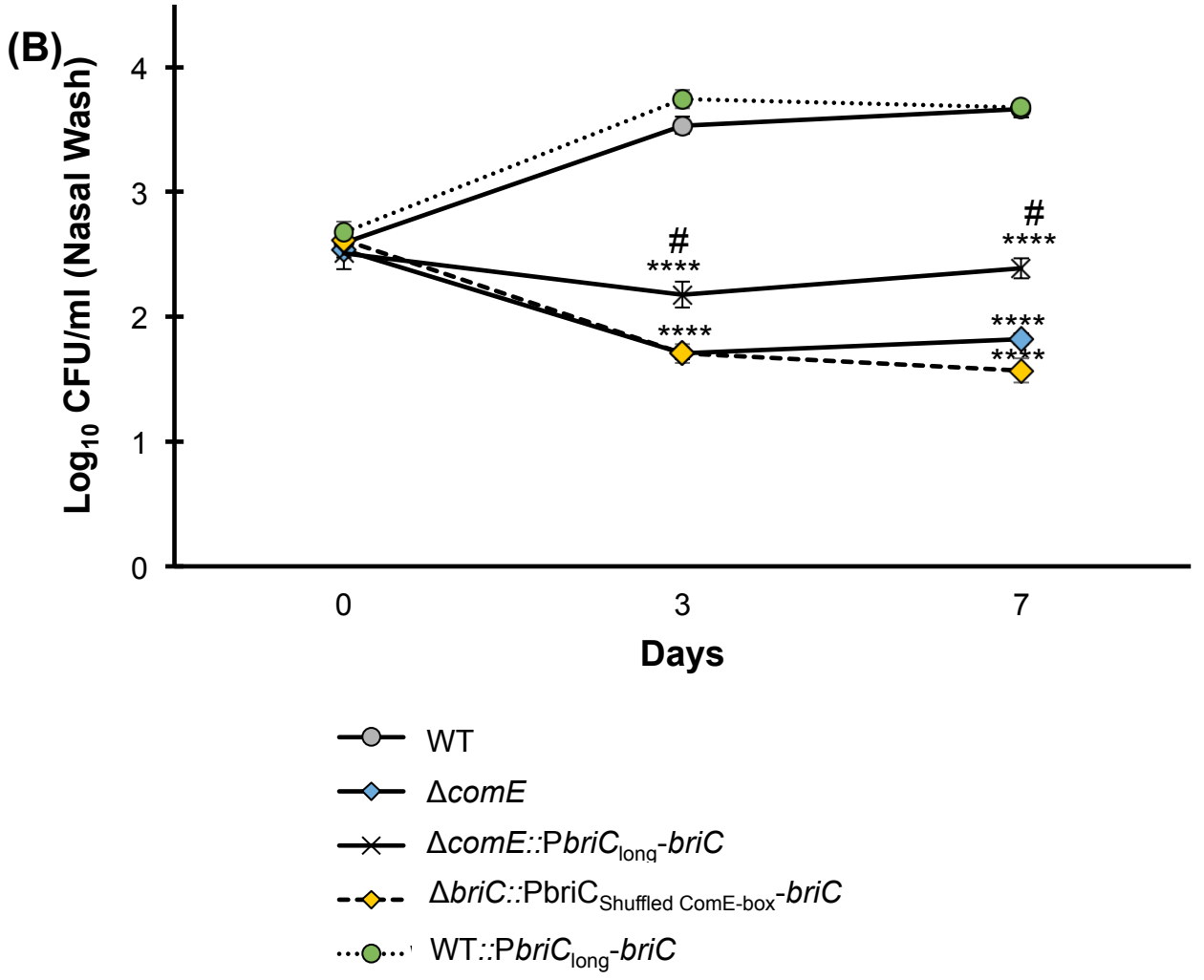
(B)
Log10 CFU/ml (Nasal Wash)
4
3
2
1
0
#
****
#
****
****
****
****
0
3
7
Days
WT
ΔcomE
ΔcomE::PbriClong-briC
ΔbriC::PbriCShuffled ComE-box-briC
WT::PbriClong-briC

Fig. 8. BriC contributes to pneumococcal colonization of the mouse nasopharynx. CD1 mice were infected intranasally with 20µl PBS containing approximately 1 X 10^5 CFU of **(A)** WT (grey circles), Δ*briC* (orange squares), and Δ*briC::briC* (black traingles) **(B)** WT (grey circles), Δ*comE* (blue diamonds), and Δ*comE::PbriC*$_{long}$-*briC* (black crosses), Δ*briC::*P*briC*$_{Shuffled\ ComE\text{-}box}$-*briC* (yellow triangles), and WT::*PbriC*$_{long}$-*briC* (green circles) cells of the pneumococcal strain D39. At predetermined time points (0, 3 & 7 days post-infection), at least five mice were culled, and the pneumococcal counts in the nasopharyngeal washes were enumerated by plating on blood agar. Y-axis represents Log_{10} counts of CFU recovered from nasal washes. X-axis represents days post-inoculation. Each data point represents the mean of data from at least five mice. Error bars show the standard error of the mean. **** $p<0.0001$ relative to the WT strain, and # $p<0.0001$ relative to the Δ*comE* strain, calculated using ANOVA and Tukey post-test.

Figure S1

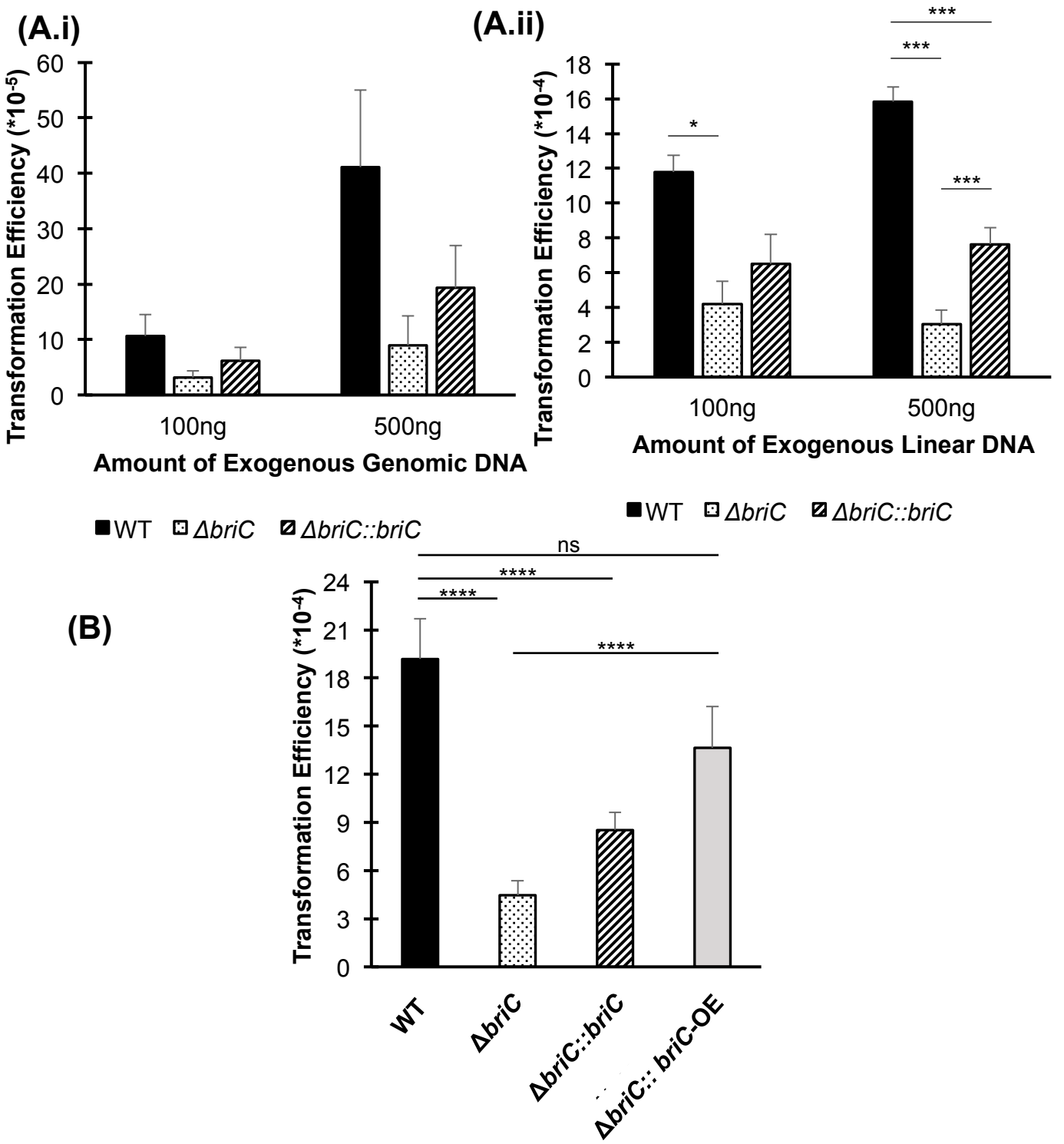

Fig. S1. BriC impacts transformation efficiency. **(A)** Transformation efficiency for WT, Δ*briC* and Δ*briC::briC* cells in strain R6D using exogenous **(i)** genomic DNA, and **(ii)** linear DNA. X-axis denotes amount of exogenous DNA added in cells. **(B)** Transformation efficiency for WT, Δ*briC*, Δ*briC::briC*, and Δ*briC::briC*-OE cells in strain R6D using 500ng of exogenous linear DNA. Y-axis denotes the fold change in transformation efficiency relative to WT cells. Cells were grown in Columbia broth at pH 6.6 to an OD_{600} of 0.05, and were treated with CSP1 along with $spec^R$ exogenous DNA for 30 minutes followed by plating on Columbia agar plates supplemented with spectinomycin (100µg/ml). No colonies were observed for samples treated with exogenous DNA in the absence of CSP1. Error bars represent standard error of the mean calculated for at least three biological replicates; 'ns' denotes not significant,* $p<0.05$, *** $p<0.001$, **** $p<0.0001$ using ANOVA followed by Tukey's post-test.